Comprehensive analysis of gene expression and DNA methylation for preeclampsia progression

Jianrong Wang*, Hongxian Song, Yanhua Zhang

Department of Obstetrics, Dongying People's Hospital, Dongying, Shandong, China

Abstract

Background: The purpose of our study is to identify novel preeclampsia (PE)-related methylation genes and uncover the molecular mechanism of PE.

Methods: All the datasets of gene expression and DNA methylation datasets for PE and normal samples were obtained from the Gene Expression Omnibus database. We first identified the differentially expressed genes (DEGs) and differential methylation genes (DMGs) between PE and normal samples followed by the functional enrichment analysis. Comprehensive analysis of DEGs and DMGs was also conducted for the identification of valuable PE-related biomarkers. The methylation validation was also performed with MassARRAY.

Results: Three DNA methylation and three gene expression datasets were incorporated. We obtained 1754 DEGs and 99 DMGs in PE samples with the thresholds of p value <0.05, $|\Delta beta| > 0.1$, and p value <0.05, respectively. Functional analysis of DEGs obtained cell adhesion molecules and leukocyte transendothelial migration. Besides, several valuable biomarkers of PE, including OCA2, CDK2AP1, and ADAM12, were identified through the integrated analysis of gene expression and DNA methylation datasets. Four methylation sites (cg03449867, cg09084244, cg09247979, and cg24194674) were validated, among which cg03449867 and cg09084244 were found to be hypermethylated and the related genes of OCA2 and CDK2AP1 were downregulated in PE compared with normal samples simultaneously. cg24194674 was hypomethylated and its correlated gene ADAM12 was upregulated in PE compared with normal samples simultaneously.

Conclusion: Our study should be helpful for the development of potential biomarkers and therapeutic targets for PE.

Keywords: Biomarkers; DNA methylation; Preeclampsia

1. INTRODUCTION

Preeclampsia (PE), a disease unique to pregnancy, is a primary health issue in pregnancies associated with a genetic influence, which is described by new-onset hypertension (blood pressure ≥140/90 mmHg) presenting after 20 weeks' gestation with clinically relevant proteinuria.[1–3] PE is a major cause of maternal and fetal mortality and morbidity, intrauterine growth restriction, preterm birth, and perinatal death.[4] At present, PE has no cure, has no robust predictive biomarkers, or has no effective therapies; the current treatment is termination of pregnancy and removing the causative organ of placenta.[5] Various attempts to identify the placental molecular pathology and seek the biomarkers of PE have not been clinically productive, because of the existence of multiple molecular subtypes of PE.[6]

Genome-wide association studies have disclosed susceptibility genes for PE. Maynard et al[7] found that soluble FMS-related tyrosine kinase-1 (FLT1) is upregulated in PE. Wang et al[8] reported methylation changes at some CpG sites of mesoderm-specific transcript (MEST) and delta-like 1 homolog (DLK1) differentially methylated regions (DMRs) in the preeclamptic group. Based on high-throughput human gene expression microarray and DNA methylation microarray, Martin et al found 123 genes with altered expression and abnormal CpG methylation. These genes (eg, *PITX2*, *SKI*, *TGFB3*, *TGIF1*, *RUNX3*, *MAPK8*, *BMP7*, *and SMAD3*) are significantly enriched in the transforming growth factor-beta (TGF-β) pathway, which is a known regulator of placental trophoblast invasion and migration.[9] However, the function between the genes is not reported in these studies, and the molecular mechanism of PE remains to be fully elucidated.

In our study, we analyzed gene expression profiling and methylation data to further investigate the molecular mechanism of PE. Genes with abnormal expression and methylation were identified, pathways and functional interactions of these genes were illustrated. To validate the reliability of DNA methylation array, we also performed the methylation validation by using MassARRAY. These results may help find potential biomarkers and benefit the prevention, detection, and treatment of PE.

2. METHODS

2.1. Datasets of methylation and gene expression profilings

Human DNA methylation microarray data of preeclamptic samples and normal samples were obtained from the Gene

*Address correspondence. Dr. Jianrong Wang, Department of Obstetrics, Dongying People's Hospital, 317, South First Road, Dongcheng, Dongying, Shandong 257091, China. E-mail address: 15505462288@163.com (J. Wang).

Author Contributions: Dr. Jianrong Wang and Dr. Hongxian Song contributed equally to this work.

Conflicts of interest: The authors declare that they have no conflicts of interest related to the subject matter or materials discussed in this article.

Journal of Chinese Medical Association. (2021) 84: 410-417.

Received November 21, 2019; accepted September 13, 2020.

doi: 10.1097/JCMA.0000000000000499.

Expression Omnibus (GEO; https://www.ncbi.nlm.nih.gov/geo/) with an accession ID of GSE75196, GSE73375, and GSE57767, as well as the corresponding human gene expression data with an accession ID of GSE54618, GSE44711, and GSE35574. The platform for GSE75196, GSE73375, and GSE57767 was GPL13534 Illumina HumanMethylation450 BeadChip (HumanMethylation450_15017482), the platform for GSE54618 and GSE44711 was GPL10558 Illumina HumanHT-12 V4.0 expression beadchip, and the platform for GSE35574 was GPL6102 Illumina human-6 v2.0 expression beadchip, respectively.

2.2. Differential methylation analysis and differentially expressed genes

There are 485,512 methylation sites in the three datasets of GSE75196, GSE73375, and GSE57767. After removing the sex chromosome, we obtained 476,932 sites. We removed the CpG sites for which beta value was not available in >80% samples and obtained 476,920 CpG sites. We performed quantile standardization due to the large gap between different datasets. The COHCAP package in R (https://sourceforge.net/projects/cohcap) was used to identify the differential methylation sites between diseases and normal tissues that are more likely to regulate downstream gene expression.[10] |Δbeta| > 0.1 and p value <0.05 were considered as differentially methylated CpG sites. Based on the gene expression of PE, we identified the aberrant DNA methylated CpG site that affected the corresponding gene expression.

Based on the gene expression microarray data, DEGs between preeclamptic and normal samples were identified using the limma package and the metaMA package analysis; the method used for the p-value combination was the inverse normal method. The adoption criterion was p value <0.05, and the differences in the expression directions were consistent in all datasets.

2.3. Functional annotation of differential methylation genes and differentially expressed genes

To acquire the biological function of the differential methylation genes (DMGs) and differentially expressed genes (DEGs), we conducted Gene Ontology (GO) and Kyoto Encyclopedia of Genes and Genomes (KEGG) pathway enrichment analysis based on the online software MetaScape (http://metascape.org/gp/index.html#/main/step1). False discovery rate (FDR) <0.05 was set as the cut-off for selecting significantly enriched functional GO and KEGG pathways.

2.4. Correlation analysis between DMGs and DEGs

We identified the genes that were not only differentially expressed but also differentially methylated to analyze the association between gene expression and DNA methylation. Methylation of DNA has been negatively correlated with gene expression in many cases. Here, we mainly identified DEGs whose expression and DNA methylation were reversely regulated in patients with PE.

2.5. Methylation validation

Six placenta tissues from three PE patients and three healthy individuals were obtained after delivery. Women who had a history of cardiovascular, renal, and other hypertension-associated diseases were excluded. This study has been approved by the ethics institute of our hospital. The signed informed consent of all the participants was obtained. We used the Sequenom MassARRAY platform (CapitalBio, Beijing, China) to perform the quantitative methylation analysis of placental tissue. This system uses matrix-assisted laser desorption/ionization time-of-flight (MALDI-TOF) mass spectrometry in combination with RNA base-specific cleavage (MassCLEAVE).[11] Primer designs for four sites of cg03449867, cg09084244, cg09247979, and cg24194674 were performed using Agena's EpiDesigner software. A 10-mer tag was added to the 5′ end of the forward primer to balance the polymerase chain reaction (PCR) conditions. The T7-promoter sequence was added to the 5′ end of the reverse primer for subsequent transcription in vitro. DNA was extracted from placenta tissues using a QIAamp DNA Mini Kit (QIAGEN) and sulfite treatment with EZ DNA Methylation Kit (ZYMO). Modified DNA amplification was performed using PCR according to the manufacturer's protocols. RNase A cleavage (MassCleave Kit; Agena Bioscience, Inc., San Diego, CA, USA) was applied for the reverse. The purified were spotted onto a 384-pad SpectroCHIP using a MassARRAYnanodispenser. Spectra peaks were obtained with a MassARRAY compact MALDI-TOF mass spectrometer. EpiTyper software was used to analyze the resulting methylation calls.

2.6. Statistical analysis

For methylation microarray datasets, the gap between different datasets is large, so we performed quantile standardization for further analysis. Then, differentially methylation analysis was performed through the software COHCAP in R package. Screening criteria were |Δbeta| > 0.1 and p value <0.05. In this analysis, two methods of t test and Wilcoxon rank sum were used to determine whether the difference in methylation levels between groups was significant.

3. RESULTS

3.1. Differential methylation analysis in PE

Totally, three datasets (GSE75196, GSE73375, and GSE57767) were included in the differential methylation analysis, and three datasets (GSE54618, GSE44711, and GSE35574) were obtained for differential gene expression analysis; the detailed information of these included datasets are listed in Tables 1 and 2. There were 99 differential methylation sites with p value <0.05 between PE and normal tissue, which include 57 hypermethylation sites and 42 hypomethylation sites. The Manhattan image of each DNA methylation site is shown in Fig. 1A. Cluster analysis between the above 99 differential methylation sites is shown in Fig. 1B. The top 20 differential methylation sites are listed in Table 3.

Table 1

Retrieval results of DNA methylation data in GEO datasets

GEO accession	Author	Platform	Samples (case:normal)	Year
GSE75196	Christine L Chiu	GPL13534 Illumina HumanMethylation450 BeadChip (HumanMethylation450_15017482)	8:16	2016
GSE73375	Rebecca Catherine Fry	GPL13534 Illumina HumanMethylation450 BeadChip (HumanMethylation450_15017482)	19:17	2015
GSE57767	Lauren Anton	GPL13534 Illumina HumanMethylation450 BeadChip (HumanMethylation450_15017482)	31:14	2014

GEO = Gene Expression Omnibus.

Table 2

Retrieval results of DNA expression data in GEO datasets

GEO accession	Platform	Samples (case:normal)	Number of genes
GSE54618	GPL10558 Illumina HumanHT-12 V4.0 expression beadchip	5:12	25,085
GSE44711	GPL10558 Illumina HumanHT-12 V4.0 expression beadchip	8:8	25,085
GSE35574	GPL6102Illumina human-6 v2.0 expression beadchip	19:40	24,335

GEO = Gene Expression Omnibus.

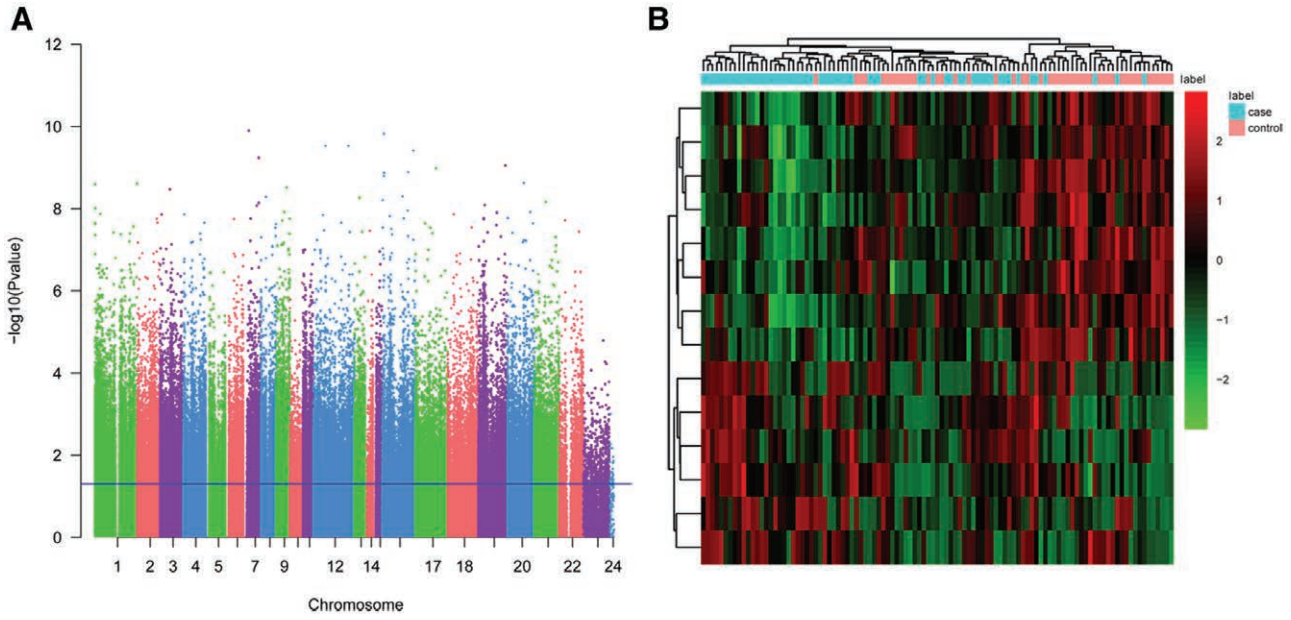

Fig. 1 Analysis of 99 differential methylation genes (DMGs) in preeclampsia (PE) compared with normal control. A, Manhattan of the 99 DMGs. B, Heatmap clustering analysis of 99 DMGs in PE compared with normal control. Row and column represent DMGs and blood samples, respectively. The color scale indicates the expression of DMGs.

Table 3

Top 20 differential methylation sites

SiteID	Gene	Island	delta.beta	*p* value	FDR
cg10689438	*GMPS*	chr3:155588009–155589602	−0.10425	1.28E−09	6.38E−05
cg07089056			−0.11997	1.11E−08	0.0002
cg24155427		chr1:31246010–31246280	−0.10463	1.35E−08	0.0002
cg08640824	*SKI*	chr1:2158212–2161173	−0.12428	4.4E−08	0.000276
cg07429087	*NMUR2*		−0.1011	5.81E−07	0.000944
cg01883425	*MDFI*	chr6:41606994–41607238	−0.10061	7.06E−07	0.001027
cg13293729			−0.10133	7.31E−07	0.001038
cg22112152			−0.10316	1.07E−06	0.001247
cg19371349	*HMGB2*	chr4:174254683–174256538	−0.10561	1.47E−06	0.001458
cg06688989	*MDFI*	chr6:41606994–41607238	−0.10051	1.54E−06	0.001499
cg15885953	*ADARB1*	chr21:46520795–46521295	0.111461	1.73E−06	0.001554
cg10321156		chr11:63685489–63685968	−0.10191	2.05E−06	0.0017
cg24643706		chr6:28602853–28603295	−0.10083	2.24E−06	0.001798
cg09918657	*MIR193B*	chr16:14395604–14397075	−0.14108	5.14E−06	0.002595
cg03475293		chr6:7051496–7052932	−0.1013	5.35E−06	0.002646
cg06637517	*DNAH1*		−0.11758	1.05E−05	0.003689
cg09157302	*SLC34A2*	chr4:25657119–25657547	−0.10764	1.21E−05	0.003925
cg08196561	*ZCCHC14*		−0.10358	1.68E−05	0.004621
cg24630825	*GPM6A*		−0.1068	2.31E−05	0.005437
cg03284308	*C16orf61; CENPN*	chr16:81040134–81041325	−0.10576	2.39E−05	0.005519

FDR = false discovery rate.

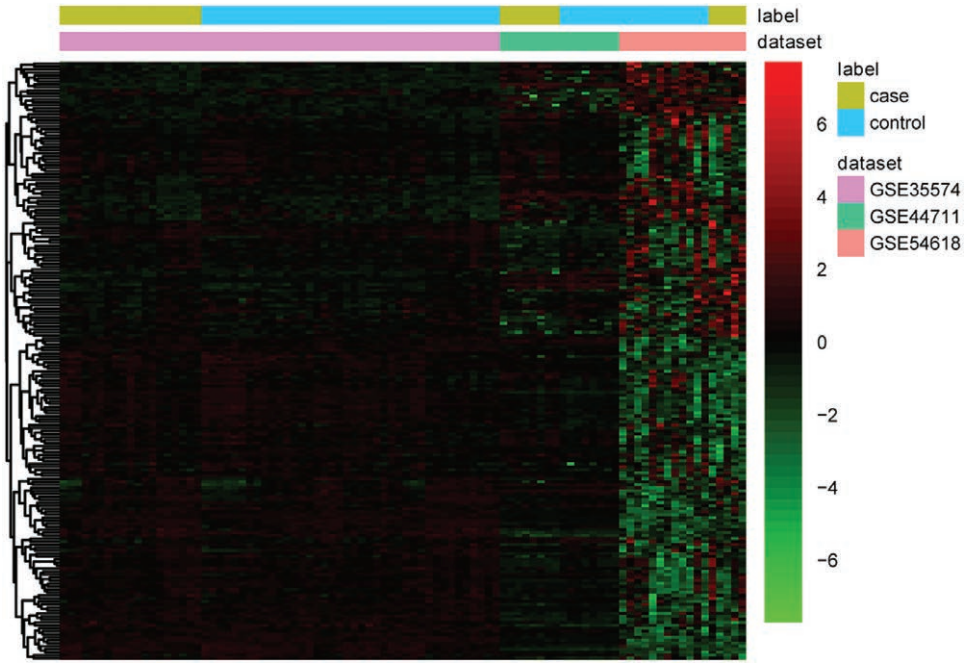

Fig. 2 Heatmap clustering analysis of top 200 differential methylation genes (DEGs) in preeclampsia (PE) compared with normal control. Row and column represent DEGs and blood samples, respectively. The color scale indicates the expression of DEGs.

3.2. DEGs in PE

For gene expression datasets, the probe corresponding to multiple genes was removed; there were 24,261 mRNAs by taking the intersection of the three datasets. Using the limma and metaMA packages for analysis, the method used for the *p*-value combination is the inverse normal method. The standard was p value <0.05, and the differential expression directions were consistent in all datasets. We also obtained 1754 DEGs. Among these genes, 840 genes were upregulated and 914 genes were downregulated. The heatmap of top 200 DEGs is shown in Fig. 2. The top 20 upregulated/downregulated genes are listed in Table 4.

Table 4

Top 20 differential expressed genes

ID	Symbol	Combined.ES	*p* value	FDR	Up or down
132160	*PPM1M*	–1.3068	1.13E–07	0.001528	Down
629	*CFB*	1.300221	1.90E–07	0.001528	Up
2162	*F13A1*	–1.3661	2.37E–07	0.001528	Down
6490	*SILV*	1.277935	2.52E–07	0.001528	Up
8263	*F8A1*	–1.24975	3.26E–07	0.001579	Down
152926	*PPM1K*	–1.25543	4.28E–07	0.001732	Down
7454	*WAS*	–1.21392	5.87E–07	0.002034	Down
6624	*FSCN1*	–1.19534	7.39E–07	0.00224	Down
170954	*KIAA1949*	–1.18704	1.15E–06	0.003091	Down
80896	*NPL*	–1.15236	1.90E–06	0.003995	Down
1515	*CTSL2*	1.155176	2.09E–06	0.003995	Up
201176	*ARHGAP27*	1.150784	2.14E–06	0.003995	Up
124961	*ZFP3*	–1.13831	2.51E–06	0.004354	Down
55466	*DNAJA4*	–1.10652	3.61E–06	0.005834	Down
23431	*AP4E1*	1.10192	4.45E–06	0.006565	Up
386757	*SLC6A10P*	1.116772	4.60E–06	0.006565	Up
254065	*BRWD3*	1.106484	5.76E–06	0.007311	Up
154141	*MBOAT1*	–1.08526	5.94E–06	0.007311	Down
3972	*LHB*	1.087587	6.23E–06	0.007311	Up

FDR = false discovery rate.

3.3. Functional enrichment of DMGs and DEGs

As the results of GO enrichment analysis (FDR < 0.05; Fig. 3A), the DMGs were significantly enriched in GO: 0021952, central nervous system projection neuron axonogenesis (log$P$ = –4.0455277178); GO: 0046332, SMAD binding (log$P$ = –3.7307493944); and GO: 0046148, pigment biosynthetic process (log$P$ = –2.9362892933). The DEGs were significantly enriched in GO: 0001816, cytokine production (log$P$ = –6.2) and GO: 0032101, regulation of response to external stimulus (log$P$ = –4.7). After KEGG analysis, we found that DEGs were enriched in leukocyte transendothelial migration (FDR = 1.35E–07) and cell adhesion molecules (CAMs; FDR = 1.11E–08), which are shown in Fig. 3B.

3.4. Association analysis between differential methylation and DEGs

Intersected analysis of DEGs and DMGs identified four overlaps, among which two genes were downregulated and hypermethylated simultaneously, that is, OCA2 and CDK2AP1. ADAM12 is upregulated and hypomethylated. Table 5 illustrates the details of those four overlaps.

3.5. Validation of the DNA methylation using MassARRAY

To validate the observations in the DNA methylation array, we detected DNA methylation change of CpGs in the four methylation regions (cg03449867, cg24194674, cg09247979, and cg09084244) using MassARRAY. As shown in Fig. 4, in total, 9, 12, 4, and 6 detectable CpG sites were examined in the methylation regions of cg03449867, cg09084244, cg09247979, and cg24194674, respectively. The percentages of methylation at four different loci were noted in PE (n = 3) and normal control (n = 3). Table 6 shows that the methylation percentage was higher in PE compared with normal control at the regions of cg03449867 and cg09084244 and was less in PE compared with normal control at the regions of cg24194674 and cg09247979. These results of DNA methylation validation were consistent with the results of DNA methylation array. Clustering analysis of these three methylation regions is shown in Fig. 5.

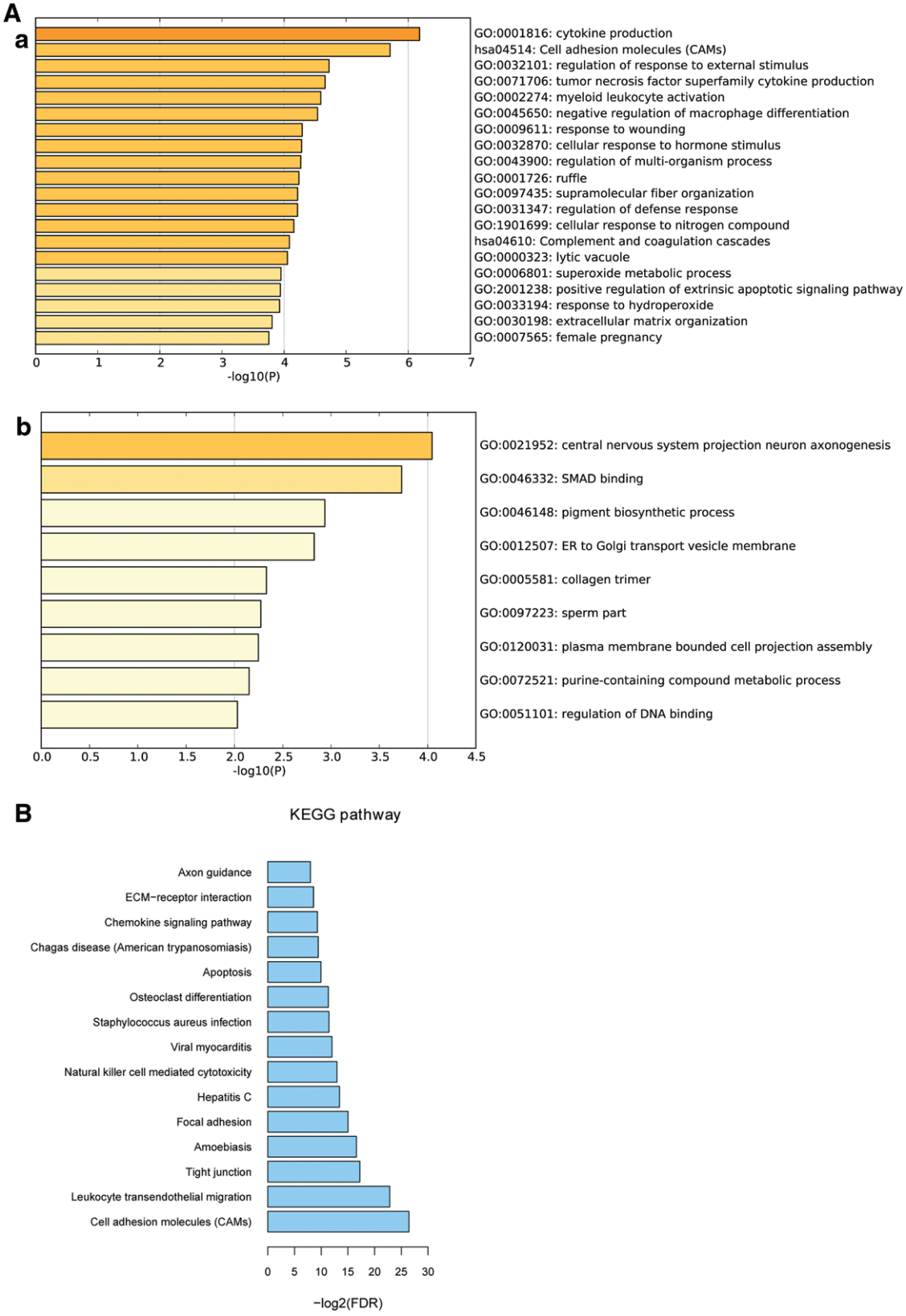

Fig. 3 A, Significantly enriched Gene Ontology (GO) terms of differential methylation genes (DMGs) and differentially expressed genes (DEGs) in preeclampsia (PE) compared with normal control: (a) DMGs and (b) DEGs. The *Y*-axis shows GO terms and the *X*-axis represents –log10 (*P*). B, Significantly enriched Kyoto Encyclopedia of Genes and Genomes (KEGG) pathways of DEGs in PE compared with normal control. The *Y*-axis shows KEGG terms and the *X*-axis represents –log2 (false discovery rate [FDR]).

Table 5

Details of differential methylation-differential expression gene

SiteID	Chr	Loc	Gene	delta.beta	*p* value	Combined.ES
cg03449867	15	28200653	OCA2	0.112347	0.028574	–0.79891
cg09084244	12	1.24E+08	CDK2AP1	0.123375	0.048909	–0.46929
cg09247979	6	1.29E+08	PTPRK	–0.14072	0.02166	–0.63404
cg24194674	10	1.28E+08	ADAM12	–0.10667	0.00185	1.071302

4. DISCUSSION

PE is a multifactorial disease, and its underlying pathogenetic mechanisms are still unclear.[12] In this study, we performed DNA methylation and gene expression analysis of PE and normal samples to identify potential biomarkers and biological pathways involved in the progression of PE. This may provide comprehensive landscape for PE which is helpful for the development of its diagnosis and treatment.[13] There were 99 differential methylation sites with p value <0.05 between PE and normal tissue, which include 57 hypermethylation sites and 42 hypomethylation sites. We also obtained 1754 DEGs. Among these genes, 840 genes were upregulated and 914 genes were

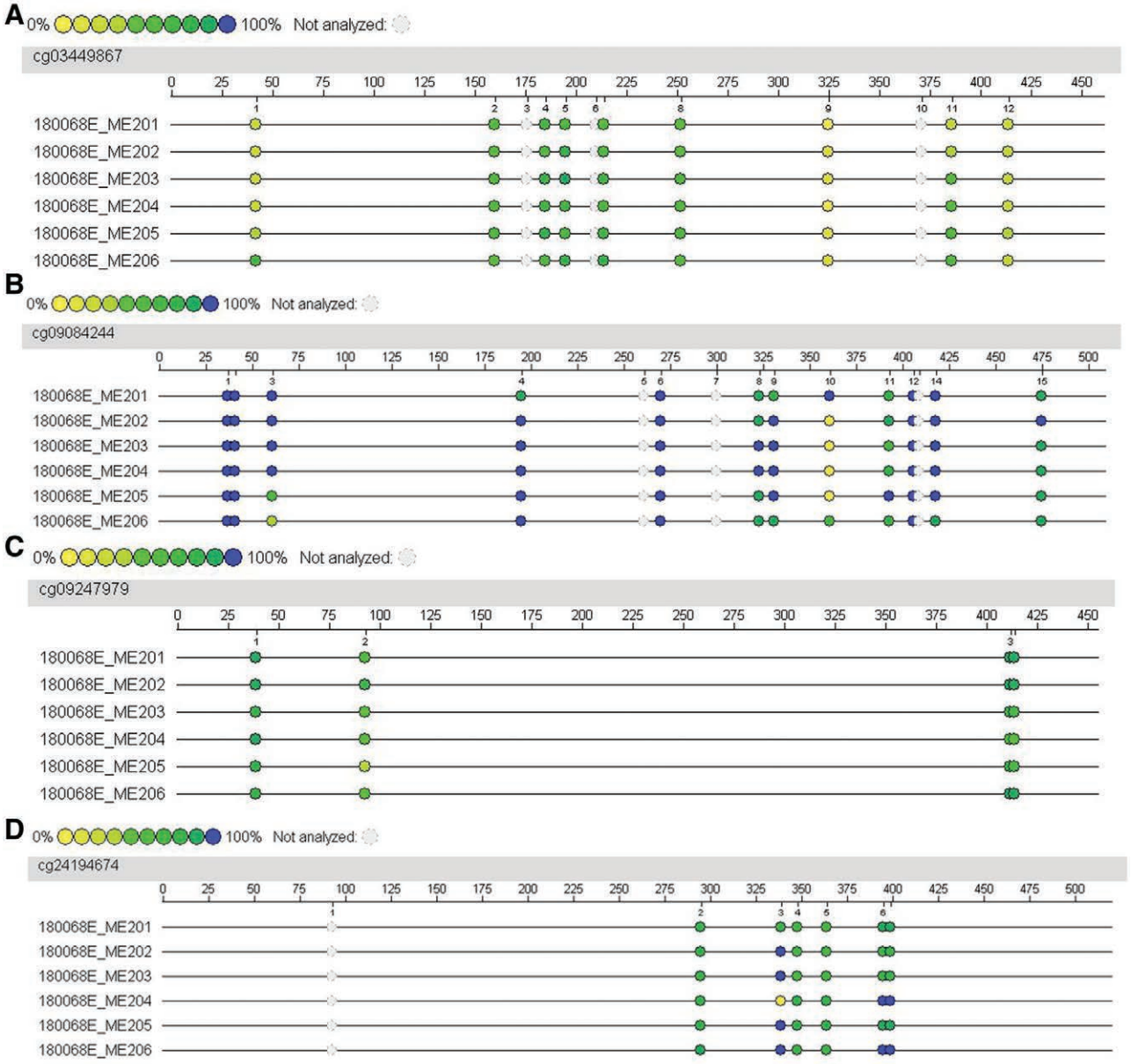

Fig. 4 Profiling of the site-specific methylation of CpG sites in the placental tissue. Matlab7.0.4 software was used to assess site-specific CpG methylation by using sequencing with sodium bisulfite treatment.

Table 6

Results of validation of DMGs

CpG	Average_Methylation_ Level_Case	SD_Methylation_ Level_Case	Average_Methylation_ Level_Control	SD_Methylation_ Level_Control	*t*_Test_*P*
cg03449867	0.481481481	0.033597717	0.433703704	0.068802215	0.166213517
cg09084244	0.836363636		0.865151515	0.037596524	0.135470065
cg09247979	0.62	0.080897741	0.721111111	0.092275754	0.395785496
cg24194674	0.771333333	0.117206371	0.749333333	0.019218047	0.746416297

DMGs = differential methylation genes.

downregulated. Intersected analysis of DEGs and DMGs identified four overlaps and the expression and methylation of three genes were consistent with four overlaps, among which OCA2 and CDK2AP1 genes were downregulated and hypermethylated simultaneously, and ADAM12 is upregulated and hypomethylated. In this study, we also validated four methylation sites, that is, cg03449867, cg09084244, cg09247979, and cg24194674, among which cg03449867 and cg09084244 were found to be hypermethylated and the related genes of OCA2 and CDK2AP1 were downregulated in PE compared with normal samples simultaneously. cg24194674 was hypomethylated and its correlated gene ADAM12 was upregulated in PE compared with normal samples simultaneously. KEGG pathways analysis of DEGs in PE compared with normal samples identified significantly enriched in CAMs and leukocyte transendothelial migration. Previous studies have found that CAMs are increased in the sera of patients with PE and that soluble CAM levels are associated with the severity of PE.[14,15] A uroproteomics study uncovered that the most differentially expressed proteins of PE are involved in CAMs pathways.[16] The concentration of glutamine in PE plasma can affect the expression of endothelial CAMs and leukocyte transmigration.[17] Factors present in the plasma of PE stimulate the transendothelial migration of neutrophils through the induction of oxidative stress and the production of interleukin (IL)-8.[18] Endothelial activation and dysfunction are central pathogenic features in women with PE, which is a multiple-system disorder during human pregnancy.[19,20] It has been suggested that PE represents an excessive maternal inflammatory response to pregnancy.

Beyond that, lysosome may play a key role in the pathogenic mechanism of PE. The hypothetical cause for PE is reduced placental perfusion and inadequate trophoblast invasion leading to endothelial dysfunction.[21,22] Renal structural and functional changes in PE, including glomerular endothelial hyperplasia, acute tubular thinning and necrosis, tubular dysfunction, and reduced renal perfusion, may lead to characteristic renal damage such as renal failure, have been described in PE.[23,24] Concentrations of the lysosomal hydrolases h-hexosaminidase (*N*-acetylglucosaminidase [NAG]) and h-galactosidase are much higher in the proximal convoluted tubule than in the distal convoluted tubule and glomerulus, and measurement of these enzymes has shown promise as a sensitive indicator of renal injury and disease.[25–27] Specifically, increased urinary h-galactosidase and h-hexosaminidase activities have been demonstrated in preeclamptic women versus nonpreeclamptic women. Jackson et al reported that PE is associated with decreased serum lysosomal hydrolase activities and elevations in the activity of acid hydrolases in urine. Changes in lysosomal hydrolase activity may permit one to discriminate between women who do and do not have PE.[28]

DNA methylation could induce gene expression repression by preventing transcription factor from binding the target regions, which represents one of the most common epigenetics. It is believed that DNA methylation plays a crucial role in

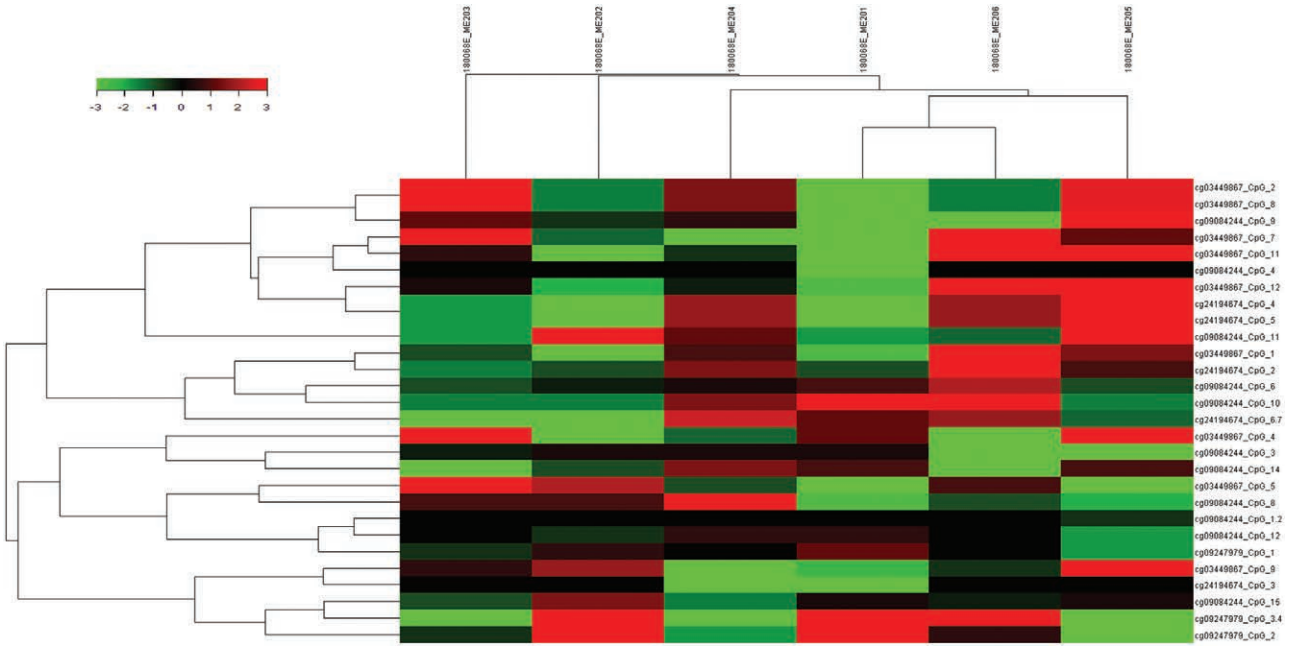

Fig. 5 Clustering analysis of three methylation regions.

PE, and several valuable methylation signatures of PE were also obtained.[29,30] ADAM12 encodes a member of a family of protein that are membrane-anchored proteins structurally related to snake venom disintegrins and participates in a variety of biological processes involving cell-cell and cell-matrix interactions, including fertilization, muscle development, and neurogenesis. Myers et al suggest that an alteration in ADAM12 may reflect an altered placental response in pregnancies subsequently complicated by PE.[31] El-Sherbiny found that ADAM12-S is significantly decreased in severe and mild PE and is correlated with cerebroplacental ratio, severity of PE, maternal complications, and fetal outcome.[32]

In conclusion, this study conducted a combined analysis of DNA methylation and gene expression profiles and identified valuable biological pathways and biomarkers for PE. Further studies are still needed for the confirmation of their roles in PE.

REFERENCES

1. Östlund E, Al-Nashi M, Hamad RR, Larsson A, Eriksson M, Bremme K, et al. Normalized endothelial function but sustained cardiovascular risk profile 11 years following a pregnancy complicated by preeclampsia. *Hypertens Res* 2013;**36**:1081–7.
2. Fabry IG, Richart T, Chengz X, Van Bortel LM, Staessen JA. Diagnosis and treatment of hypertensive disorders during pregnancy. *Acta Clin Belg* 2010;**65**:229–36.
3. Roberts JM, Pearson G, Cutler J, Lindheimer M; NHLBI Working Group on Research on Hypertension During Pregnancy. Summary of the NHLBI Working Group on research on hypertension during pregnancy. *Hypertension* 2003;**41**:437–45.
4. Poon LC, Kametas NA, Maiz N, Akolekar R, Nicolaides KH. First-trimester prediction of hypertensive disorders in pregnancy. *Hypertension* 2009;**53**:812–8.
5. Leavey K, Wilson SL, Bainbridge SA, Robinson WP, Cox BJ. Epigenetic regulation of placental gene expression in transcriptional subtypes of preeclampsia. *Clin Epigenetics* 2018;**10**:28.
6. Leavey K, Bainbridge SA, Cox BJ. Large scale aggregate microarray analysis reveals three distinct molecular subclasses of human preeclampsia. *PLoS One* 2015;**10**:e0116508.
7. Maynard SE, Min JY, Merchan J, Lim KH, Li J, Mondal S, et al. Excess placental soluble fms-like tyrosine kinase 1 (sFlt1) may contribute to endothelial dysfunction, hypertension, and proteinuria in preeclampsia. *J Clin Invest* 2003;**111**:649–58.
8. Wang X, Wan L, Weng X, Xie J, Zhang A, Liu Y, et al. Alteration in methylation level at differential methylated regions of MEST and DLK1 in fetus of preeclampsia. *Hypertens Pregnancy* 2018;**37**:1–8.
9. Martin E, Ray PD, Smeester L, Grace MR, Boggess K, Fry RC. Epigenetics and preeclampsia: defining functional epimutations in the preeclamptic placenta related to the TGF-β pathway. *PLoS One* 2015;**10**:e0141294.
10. Warden CD, Lee H, Tompkins JD, Li X, Wang C, Riggs AD, et al. COHCAP: an integrative genomic pipeline for single-nucleotide resolution DNA methylation analysis. *Nucleic Acids Res* 2013;**41**:e117.
11. Wang L, Wang F, Guan J, Le J, Wu L, Zou J, et al. Relation between hypomethylation of long interspersed nucleotide elements and risk of neural tube defects. *Am J Clin Nutr* 2010;**91**:1359–67.
12. Soellner L, Kopp KM, Mütze S, Meyer R, Begemann M, Rudnik S, et al. NLRP genes and their role in preeclampsia and multi-locus imprinting disorders. *J Perinat Med* 2018;**46**:169–73.
13. Fang G, Zhang QH, Tang Q, Jiang Z, Xing S, Li J, et al. Comprehensive analysis of gene expression and DNA methylation datasets identify valuable biomarkers for rheumatoid arthritis progression. *Oncotarget* 2018;**9**:2977–83.
14. Djurovic S, Schjetlein R, Wisløff F, Haugen G, Berg K. Increased levels of intercellular adhesion molecules and vascular cell adhesion molecules in pre-eclampsia. *Br J Obstet Gynaecol* 1997;**104**:466–70.
15. Coata G, Pennacchi L, Bini V, Liotta L, Di Renzo GC. Soluble adhesion molecules: marker of pre-eclampsia and intrauterine growth restriction. *J Matern Fetal Neonatal Med* 2002;**12**:28–34.
16. Ding W, Qiu B, Cram DS, Chen X, Li S, Zhou X, et al. Isobaric tag for relative and absolute quantitation based quantitative proteomics reveals unique urinary protein profiles in patients with preeclampsia. *J Cell Mol Med* 2019;**23**:5822–6.
17. Hsu CS, Chou SY, Liang SJ, Chang CY, Yeh CL, Yeh SL. Effect of glutamine on cell adhesion molecule expression and leukocyte transmigration in endothelial cells stimulated by preeclamptic plasma. *Nutrition* 2005;**21**:1134–40.
18. Walsh SW. Plasma from preeclamptic women stimulates transendothelial migration of neutrophils. *Reprod Sci* 2009;**16**:320–5.
19. Roberts JM, Taylor RN, Musci TJ, Rodgers GM, Hubel CA, McLaughlin MK. Preeclampsia: an endothelial cell disorder. *Am J Obstet Gynecol* 1989;**161**:1200–4.
20. Redman CW, Sacks GP, Sargent IL. Preeclampsia: an excessive maternal inflammatory response to pregnancy. *Am J Obstet Gynecol* 1999;**180**(2 Pt 1):499–506.
21. Friedman SA, Taylor RN, Roberts JM. Pathophysiology of preeclampsia. Clin Perinatol 1990;**14**:147.
22. Meekins JW, Pijnenborg R, Hanssens M, McFadyen IR, van Asshe A. A study of placental bed spiral arteries and trophoblast invasion in normal and severe pre-eclamptic pregnancies. *Br J Obstet Gynaecol* 1994;**101**:669–74.
23. Isler CM, Martin JN Jr. Preeclampsia: pathophysiology and practice considerations for the consulting nephrologist. *Semin Nephrol* 2002;**22**:54–64.
24. Sturgiss SN, Dunlop W, Davison JM. Renal haemodynamics and tubular function in human pregnancy. *Baillieres Clin Obstet Gynaecol* 1987;**1**:769–87.
25. Le Hir M, Dubach UC, Schmidt U. Quantitative distribution of lysosomal hydrolases in the rat nephron. *Histochemistry* 1979;**63**:245–51.
26. Dance N, Price RG, Cattell WR, Lansdell J, Richards B. The excretion of N-acetyl-beta-glucosaminidase and beta-galactosidase by patients with renal disease. *Clin Chim Acta* 1970;**27**:87–92.
27. Guder WG, Hofmann W. Markers for the diagnosis and monitoring of renal tubular lesions. *Clin Nephrol* 1992;**38**(Suppl 1):S3–7.
28. Jackson DW, Sciscione A, Hartley TL, Haynes AL, Carder EA, Blakemore KJ, et al. Lysosomal enzymuria in preeclampsia. *Am J Kidney Dis* 1996;**27**:826–33.
29. Anderson CM, Ralph JL, Wright ML, Linggi B, Ohm JE. DNA methylation as a biomarker for preeclampsia. *Biol Res Nurs* 2014;**16**:409–20.
30. Blair JD, Langlois S, McFadden DE, Robinson WP. Overlapping DNA methylation profile between placentas with trisomy 16 and early-onset preeclampsia. *Placenta* 2014;**35**:216–22.
31. Myers JE, Thomas G, Tuytten R, Van Herrewege Y, Djiokep RO, Roberts CT, et al. Mid-trimester maternal ADAM12 levels differ according to fetal gender in pregnancies complicated by preeclampsia. *Reprod Sci* 2015;**22**:235–41.
32. El-Sherbiny W, Nasr A, Soliman A. Metalloprotease (ADAM12-S) as a predictor of preeclampsia: correlation with severity, maternal complications, fetal outcome, and Doppler parameters. *Hypertens Pregnancy* 2012;**31**:442–50.